# Concentration Method of Edge Detection
# A Detection Theoretic Analysis

August 27, 2007

## Contents

# 1 Concentration Method of Edge Detection

## 1.1 Principle

Let $f(x)$ be a $2\pi$ periodic piecewise smooth function in $[-\pi, \pi)$. If $f(x^+)$ and $f(x^-)$ are the right and left hand limits respectively of the function $f(x)$ at any point $x$, the corresponding jump function $[f](x)$ is defined as

$$[f](x) := f(x^+) - f(x^-)$$

$[f](x)$ gives the location of edges in the function $f(x)$. The concentration method of edge detection is a method of computing the jump function from the Fourier coefficients of $f(x)$. This makes the method suitable for processes where Fourier coefficients are available as input data, such as Magnetic Resonance Imaging.

Given the (continuous) Fourier coefficients $\hat{f}_l \quad l \in [-N, N]$ of the function $f(x)$, it is shown in [2] that the generalized conjugate partial Fourier sum

$$S_N^\sigma[f](x) = i \sum_{l=-N}^{N} \hat{f}_l \operatorname{sgn}(l)\, \sigma(\frac{|l|}{N})\, e^{ilx} \tag{1}$$

converges to the jump function or "concentrates" near the edges of $f(x)$, with the rate of convergence determined by the "concentration factor" $\sigma_{l,N}(\eta) = \sigma(\frac{|l|}{N})$.

Fig 1 shows an example of this method. $f(x)$ is a periodic ramp function defined as

$$f(x) = \begin{cases} \dfrac{x+\pi}{2} & x < 0 \\ \dfrac{x-\pi}{2} & x > 0 \end{cases}$$

The corresponding jump function is

$$[f](x) = \begin{cases} -\pi & x = 0 \\ 0 & \text{otherwise} \end{cases}$$

A value of $N = 32$ was used for the jump function approximation along with the Gibbs concentration factor, which is introduced in the next section.

## 1.2 Concentration Factors

The following conditions, detailed in [2] are required for a concentration factor, $\sigma_{l,N}(\eta) = \sigma(\frac{|l|}{N})$ to be admissible,

1. $\tilde{K}_N(x) = \displaystyle\sum_{l=1}^{N} \sigma(\frac{|l|}{N}) \sin(lx)$ is odd
2. $\displaystyle\lim_{N\to\infty} \int_0^\pi \tilde{K}_N(x)dx \to -1$
3. $\dfrac{\sigma(\eta)}{\eta} = \dfrac{\sigma(|l|/N)}{|l|/N} \in C^2(0,1)$

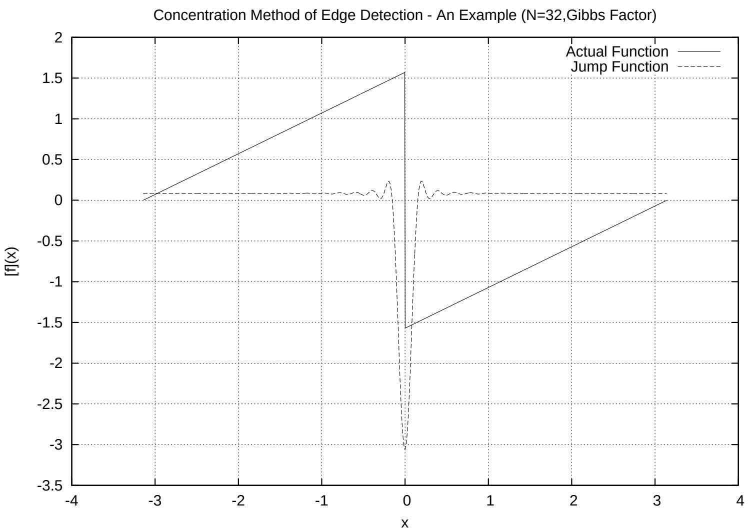


Figure 1: Concentration method - An Example ($N = 32$, Gibbs Concentration Factor)

Although one can come up with an infinite number of concentration factors which satisfy the admissibility criteria, certain factors have been well studied ([2], [3]) and documented. Chief among these are the Gibbs, Polynomial and Exponential concentration factors. The Gibbs and Polynomial factors have the added feature of being representative of some physical space process. The Gibbs factor recreates physical space divided differences while the $p^{th}$ order Polynomial factor is equivalent to an order $p$ differentiated Fourier partial sum. Table 1 gives the expressions for these concentration factors.

| **Factor** | **Expression** | **Remarks** |
|---|---|---|
| Gibbs | $\sigma_G(\eta) = \dfrac{\pi \sin(\pi\eta)}{Si(\pi)}$ | $Si(\pi) = \displaystyle\int_0^\pi \frac{\sin(x)}{x}\,dx$ |
| Polynomial | $\sigma_P(\eta) = -p\pi\eta^p$ | $p$ is the order of the factor |
| Exponential | $\sigma_E(\eta) = Const.\eta \exp\left(\dfrac{1}{\alpha\eta(\eta-1)}\right)$ | $\alpha$ is the order<br>$Const$ is a normalizing constant<br>$Const = \dfrac{\pi}{\int_{\frac{1}{N}}^{1-\frac{1}{N}} \exp\left(\frac{1}{\alpha\tau(\tau-1)}\right) d\tau}$ |

Table 1: Popular Concentration Factors

The choice of concentration factor decides the tradeoff between convergence away from the jump discontinuity and the resolution at the edge location. This is illustrated in Fig. 2 where the step response of the three concentration factors mentioned in Table 1 is plotted.

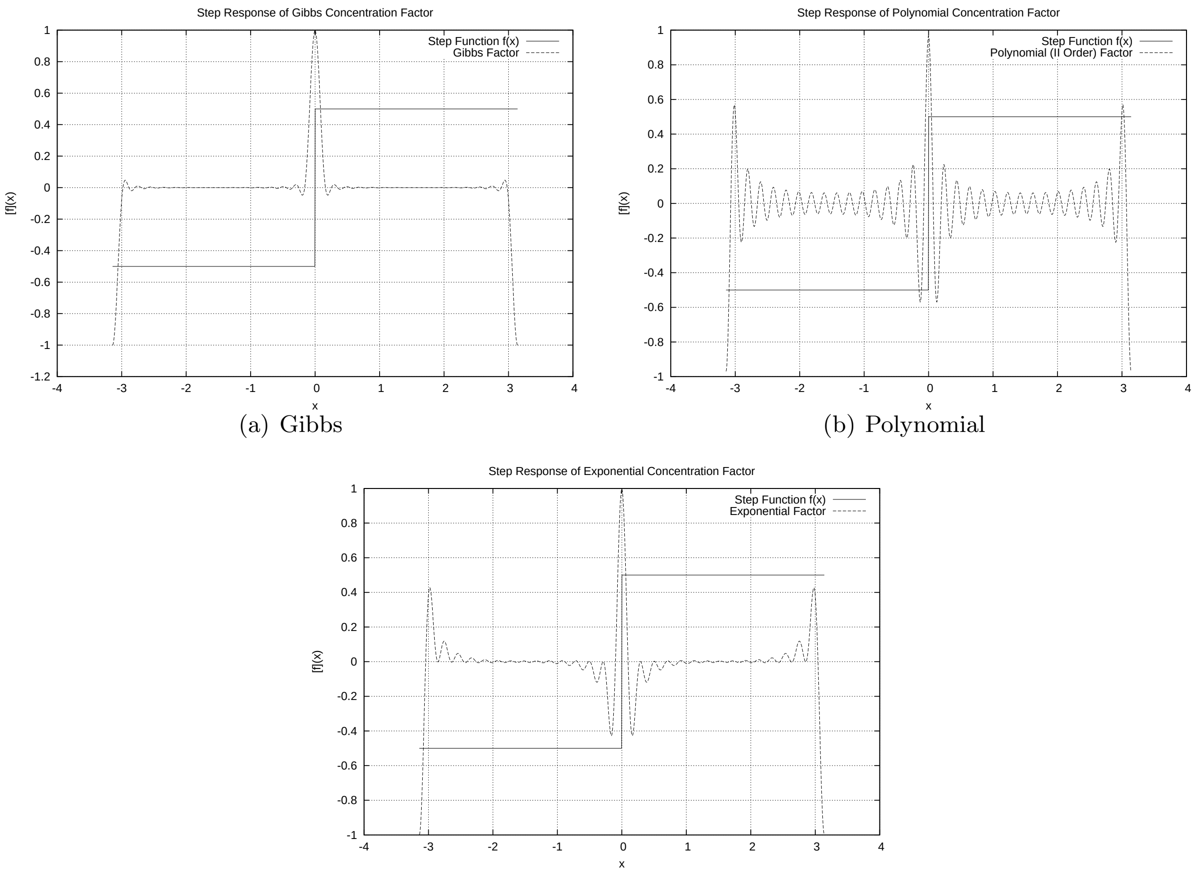


(a) Gibbs (b) Polynomial

(c) Exponential

Figure 2: Step Response of Different Concentration Factors ($N = 32$)

## 1.3 Interpretation as a Filtering Operation

Using Eq. 1 and Fourier transform properties, we may interpret the concentration method as a form of filtering, where the Fourier space filter coefficients are given by

$$h_l = i\,\mathrm{sgn}(l)\,\sigma(\frac{|l|}{N}) \quad l \in [-N, N]$$

The equivalent physical space "impulse response" is the concentration kernel

$$h(x) = \sum_{l=-N}^{N} \left( i\,\mathrm{sgn}(l)\,\sigma(\frac{|l|}{N}) \right) e^{ilx}$$

Therefore, we have

$$S_N^\sigma[f](x) = f(x) * h(x)$$

As an example, the filter coefficients $h_l$ (Magnitude) and the concentration kernel $h(x)$ are plotted in Figs. 3 and 4.

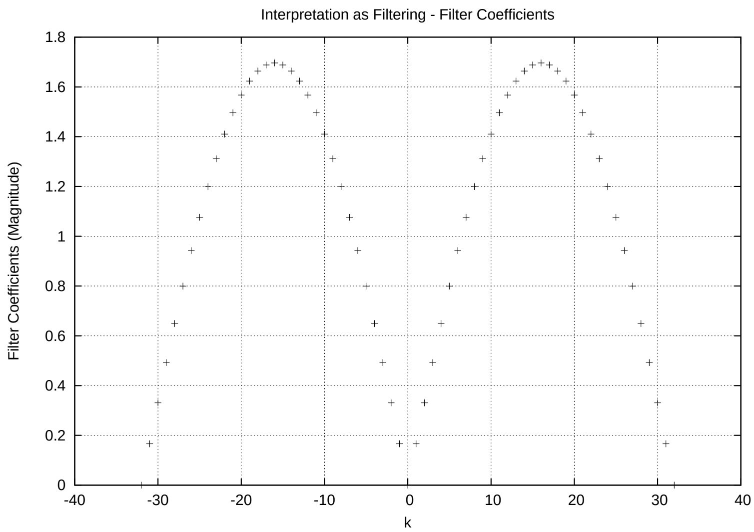


Figure 3: Interpretation as Filtering - Filter Coefficients $h_l$ (Gibbs Factor, $N = 32$)

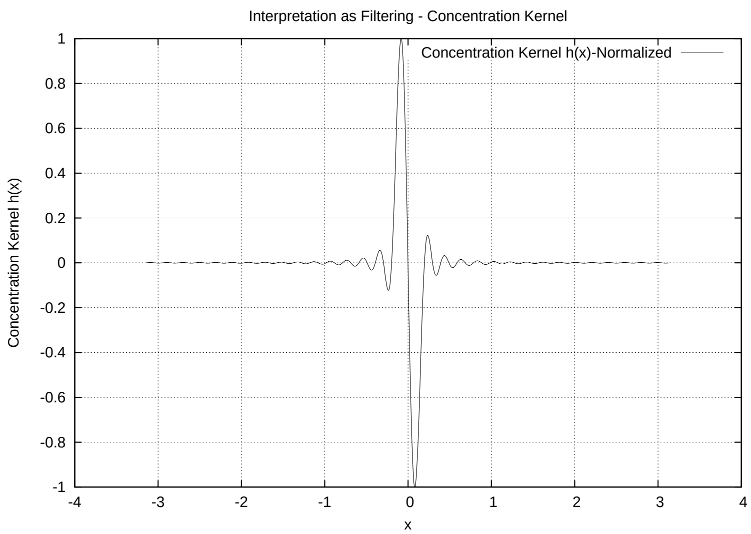


Figure 4: Interpretation as Filtering - Concentration Kernel $h(x)$ (Gibbs Factor, $N = 32$)

### 1.4 Building a Detector

Since $S_N^\sigma[f](x)$ in Eq. 1 satisfies the relation ([3])

$$S_N^\sigma[f](x) = [f](x) + \mathcal{O}(\epsilon)$$

where $\epsilon$ represents a small scale, we may build a simple detector by comparing $S_N^\sigma[f](x)$ to a threshold $T$. Other (nonlinear) methods such as enhancement of scales [3] and the minmod method [4] may also be used to build enhanced edge detectors enjoying better resolution and accuracy.

## 2 Statistical Properties of the Jump Function

It is assumed that the true Fourier coefficients $\hat{f}_l$ are corrupted by Zero Mean Additive White Gaussian Noise (ZMAWGN) of variance $\rho^2$ to yield the observed coefficients $\hat{\mathbf{g}}_l$[1]. Let $\hat{\mathbf{n}}_l$ denote the noise coefficients. Hence

$$\hat{\mathbf{g}}_l = \hat{f}_l + \hat{\mathbf{n}}_l \quad l \in [-N, N]$$

Applying the concentration method yields,

$$\begin{aligned}
S_N^\sigma[\mathbf{g}](x) &= i \sum_{l=-N}^{N} \hat{\mathbf{g}}_l \operatorname{sgn}(l)\, \sigma(\frac{|l|}{N})\, e^{ilx} \\
&= i \sum_{l=-N}^{N} (\hat{f}_l + \hat{\mathbf{n}}_l) \operatorname{sgn}(l)\, \sigma(\frac{|l|}{N})\, e^{ilx} \\
S_N^\sigma[\mathbf{g}](x) &= i \sum_{l=-N}^{N} \hat{f}_l \operatorname{sgn}(l)\, \sigma(\frac{|l|}{N})\, e^{ilx} + i \sum_{l=-N}^{N} \hat{\mathbf{n}}_l \operatorname{sgn}(l)\, \sigma(\frac{|l|}{N})\, e^{ilx} \qquad (2) \\
&= S_N^\sigma[f](x) + S_N^\sigma[\mathbf{n}](x)
\end{aligned}$$

### 2.1 Expression for the Mean

$$\begin{aligned}
E\left[S_N^\sigma[\mathbf{g}](x)\right] &= E\left[ i \sum_{l=-N}^{N} \hat{f}_l \operatorname{sgn}(l)\, \sigma(\frac{|l|}{N})\, e^{ilx} + i \sum_{l=-N}^{N} \hat{\mathbf{n}}_l \operatorname{sgn}(l)\, \sigma(\frac{|l|}{N})\, e^{ilx} \right] \\
&= E\left[ i \sum_{l=-N}^{N} \hat{f}_l \operatorname{sgn}(l)\, \sigma(\frac{|l|}{N})\, e^{ilx} \right] + E\left[ i \sum_{l=-N}^{N} \hat{\mathbf{n}}_l \operatorname{sgn}(l)\, \sigma(\frac{|l|}{N})\, e^{ilx} \right] \\
&= i \sum_{l=-N}^{N} E[\hat{f}_l] \operatorname{sgn}(l)\, \sigma(\frac{|l|}{N})\, e^{ilx} + i \sum_{l=-N}^{N} E[\hat{\mathbf{n}}_l] \operatorname{sgn}(l)\, \sigma(\frac{|l|}{N})\, e^{ilx}
\end{aligned} \qquad (3)$$

Since $E[\hat{\mathbf{n}}_l] = 0$, and $f_l$ is deterministic,

$$E\left[S_N^\sigma[\mathbf{g}](x)\right] = i \sum_{l=-N}^{N} \hat{f}_l \operatorname{sgn}(l)\, \sigma(\frac{|l|}{N})\, e^{ilx} \qquad (4)$$

Hence the noise component does not bias the resulting jump function approximation.

[1]Bold face fonts represents random quantities while normal face fonts represents deterministic quantities.

### 2.2 Expression for the Covariance

Although the noise component in physical space remains Gaussian (due to the linear nature of the concentration method), it is clear that the convolution with the concentration kernel causes the noise to become coloured. Detectors to be considered later will employ multiple data points from the jump function $S_N^\sigma[\mathbf{g}](x)$ and/or multiple concentation factors. Hence, the noise component will be described by a covariance matrix. In this regard, it is useful to compute an expression for each element of the covariance matrix as follows,

Since the mean of the noise component is zero,

$$\begin{aligned}
(C_\mathbf{n})_{p,q}^{x_a,x_b} &= E\left[(S_N^{\sigma_p}[\mathbf{n}](x_a))(S_N^{\sigma_q}[\mathbf{n}](x_b))^*\right] \\
&= E\left[\left(i\sum_{l=-N}^{N}\hat{\mathbf{n}}_l\,\mathrm{sgn}(l)\,\sigma_p(\frac{|l|}{N})\,e^{ilx_a}\right)\left(-i\sum_{m=-N}^{N}\hat{\mathbf{n}}_m^*\,\mathrm{sgn}(m)\,\sigma_q(\frac{|m|}{N})\,e^{-imx_b}\right)\right] \\
&= E\left[\sum_{l=-N}^{N}|\hat{\mathbf{n}}_l|^2\sigma_p(\frac{|l|}{N})\sigma_q(\frac{|l|}{N})\,e^{il(x_a-x_b)}\right] \\
&\quad +E\left[\sum_{m=-N}^{N}\sum_{l=-N}^{N}\hat{\mathbf{n}}_m^*\,\hat{\mathbf{n}}_l\,\mathrm{sgn}(m)\,\mathrm{sgn}(l)\,\sigma_q(\frac{|m|}{N})\,\sigma_p(\frac{|l|}{N})\,e^{-imx_b}e^{ilx_a}\right] \\
&= \sum_{l=-N}^{N}E[|\hat{\mathbf{n}}_l|^2]\,\sigma_p(\frac{|l|}{N})\,\sigma_q(\frac{|l|}{N})\,e^{il(x_a-x_b)} \\
&\quad +\sum_{m=-N}^{N}\sum_{l=-N}^{N}E[\hat{\mathbf{n}}_m^*\,\hat{\mathbf{n}}_l]\,\mathrm{sgn}(m)\,\mathrm{sgn}(l)\,\sigma_q(\frac{|m|}{N})\,\sigma_p(\frac{|l|}{N})\,e^{-imx_b}e^{ilx_a}
\end{aligned}$$

Since $\mathbf{n}_l \quad l\in[-N,N]$ are independent and zero mean variates , $E[\hat{\mathbf{n}}_m^*\,\hat{\mathbf{n}}_l] = E[\hat{\mathbf{n}}_m^*]\,E[\hat{\mathbf{n}}_l] = 0$. Hence the second term in the above expression goes to zero. Further, $E[|\hat{\mathbf{n}}_l|^2] = \rho^2$ and,

$$(C_\mathbf{n})_{p,q}^{x_a,x_b} = \rho^2\sum_{l=-N}^{N}\sigma_p(\frac{|l|}{N})\sigma_q(\frac{|l|}{N})e^{il(x_a-x_b)} \tag{5}$$

## 3 Design and Performance of an Optimum Detector

The detector to be constructed will take either a scalar value ($\mathbf{y}$) or a vector of data points ($\mathbf{Y}$) from the jump function approximation ($S_N^\sigma[\mathbf{g}](x)$) and decide on one of the following hypothesis - $\mathcal{H}_0$ (Edge Absent) or $\mathcal{H}_1$ (Edge Present).

### 3.1 Scalar Case

#### 3.1.1 Detector Design

It is customary to start the design and analysis by statistically characterizing the data under either hypothesis. We shall first consider building a detector using a single scalar value, $\mathbf{y} = [\mathbf{g}](x)$. Consider the test function,

$$f(x) = \begin{cases} -0.5 & x<0 \\ +0.5 & x\geq 0 \end{cases}$$

For simplicity of analysis, this test function has a single edge at $x = 0$. The corresponding jump function is

$$[f](x) = \begin{cases} 1 & x = 0 \\ 0 & \text{otherwise} \end{cases}$$

When no edge is present, $[f](x) = 0$. From the analysis in Section 2, the only contribution is the Gaussian noise whose mean is zero and variance[2] $\tilde{\rho}^2 = \rho^2 \sum_{l=-N}^{N} \left[\sigma(\frac{|l|}{N})\right]^2$ (i.e., $\mathcal{N}[0, \tilde{\rho}^2]$). Similarly, it can be shown that in the presence of an edge, $\mathbf{y} = [\mathbf{g}](x)$ is $\mathcal{N}[1, \tilde{\rho}^2]$. Hence, we may define the two hypotheses, $\mathcal{H}_0$ and $\mathcal{H}_1$ as follows,

$$\mathcal{H}_0 : \quad \mathbf{y} = \mathbf{n}$$

$$\mathcal{H}_1 : \quad \mathbf{y} = 1 + \mathbf{n}$$

Also,

$$f_{\mathbf{y}}(y|\mathcal{H}_0) = \mathcal{N}[0, \tilde{\rho}^2]$$
$$f_{\mathbf{y}}(y|\mathcal{H}_1) = \mathcal{N}[1, \tilde{\rho}^2]$$

We use the Neyman Pearson criterion [1] for designing the detector, which maximizes the Detection Probability $P_D$ for a given False Alarm Probability $P_{FA}$. The optimal detector for this case is given by

$$\rightarrow \mathcal{H}_1 : \quad \frac{f_{\mathbf{y}}(y|\mathcal{H}_1)}{f_{\mathbf{y}}(y|\mathcal{H}_0)} > \gamma$$

$$\begin{aligned} \frac{\frac{1}{\sqrt{2\pi\tilde{\rho}^2}} \exp\left[-\frac{(y-1)^2}{2\tilde{\rho}^2}\right]}{\frac{1}{\sqrt{2\pi\tilde{\rho}^2}} \exp\left[-\frac{y^2}{2\tilde{\rho}^2}\right]} &> \gamma \\ \text{or } \exp\left[-\frac{(y-1)^2}{2\tilde{\rho}^2}\right] \exp\left[\frac{y^2}{2\tilde{\rho}^2}\right] &> \gamma \\ \exp\left[\frac{y}{\tilde{\rho}^2}\right] \exp\left[-\frac{1}{2\tilde{\rho}^2}\right] &> \gamma \end{aligned}$$

Incorporating the data independent term $e^{-\frac{1}{2\tilde{\rho}^2}}$ into the threshold

$$\begin{aligned} \exp\left[\frac{y}{\tilde{\rho}^2}\right] &> \bar{\gamma} \\ \frac{y}{\tilde{\rho}^2} &> \ln \bar{\gamma} \\ \text{or } \rightarrow \mathcal{H}_1 : \quad y &> \dot{\gamma} \text{ where } \dot{\gamma} = \tilde{\rho}^2 \ln \bar{\gamma} \end{aligned}$$

[2]The variance depends on whether we consider the real or absolute value of $[g](x)$ (or $S_N^\sigma[\mathbf{g}](x)$).
If $S_N^\sigma[\mathbf{g}](x) = \Re\text{e}\left[i \sum_{l=-N}^{N} \hat{\mathbf{g}}_l \,\text{sgn}(l)\, \sigma(\frac{|l|}{N})\, e^{ilx}\right]$, $\tilde{\rho}^2 = \frac{\rho^2}{2} \sum_{l=-N}^{N} \left[\sigma(\frac{|l|}{N})\right]^2$
If $S_N^\sigma[\mathbf{g}](x) = \left|i \sum_{l=-N}^{N} \hat{\mathbf{g}}_l \,\text{sgn}(l)\, \sigma(\frac{|l|}{N})\, e^{ilx}\right|$, $\tilde{\rho}^2 = \rho^2 \sum_{l=-N}^{N} \left[\sigma(\frac{|l|}{N})\right]^2$

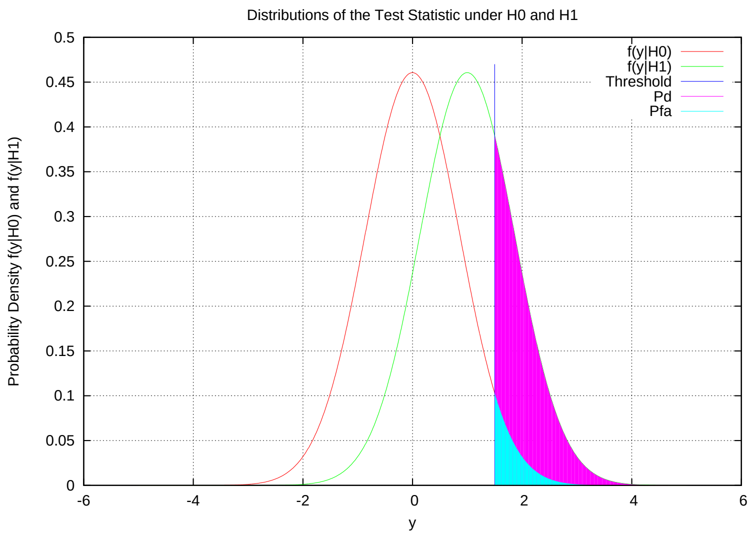


Figure 5: Probability Distribution of the Test Statistic under $\mathcal{H}_0$ and $\mathcal{H}_1$

### 3.1.2 Performance of the Detector

For this scalar case, the distribution of the test statistic $TS = \mathbf{y}$ (Fig. 5) is obviously the same as that of the data sample. Hence we may write,

$$\begin{aligned} P_{FA} &= \int_{\dot{\gamma}}^{\infty} f_{\mathbf{y}}(y|\mathcal{H}_0)dy \\ &= \int_{\dot{\gamma}}^{\infty} \frac{1}{\sqrt{2\pi\tilde{\rho}^2}} \exp\left[-\frac{y^2}{2\tilde{\rho}^2}\right] dy \\ &= Q\left(\frac{\dot{\gamma}}{\tilde{\rho}}\right) \end{aligned} \tag{6}$$

where $Q(.)$ is the right tail probability of a standard normal pdf, i.e., $Q(x) = \dfrac{1}{\sqrt{2\pi}} \displaystyle\int_x^{\infty} e^{-\frac{t^2}{2}} dt$.

Similarly, we may write,

$$\begin{aligned} P_D &= \int_{\dot{\gamma}}^{\infty} f_{\mathbf{y}}(y|\mathcal{H}_1)dy \\ &= \int_{\dot{\gamma}}^{\infty} \frac{1}{\sqrt{2\pi\tilde{\rho}^2}} \exp\left[-\frac{(y-1)^2}{2\tilde{\rho}^2}\right] dy \\ &= Q\left(\frac{\dot{\gamma}-1}{\tilde{\rho}}\right) \end{aligned} \tag{7}$$

Using Equations 6 and 7, we may write [3]

$$P_D = Q\left(\frac{Q^{-1}(P_{FA})\tilde{\rho} - 1}{\tilde{\rho}}\right)$$

[3] Q(.) is an invertible function

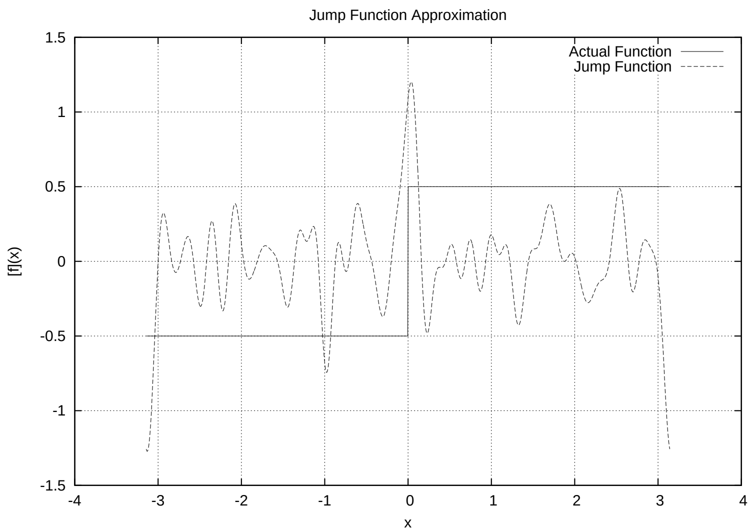


Figure 6: Jump Function Approximation ($N = 32$, Polynomial Concentration Factor, $\rho^2 = 1.5$)

$$P_D \quad = \quad Q\left(Q^{-1}(P_{FA}) - \sqrt{\frac{1}{\tilde{\rho}^2}}\right) \tag{8}$$

A good detector is one which obtains a high Probability of Detection ($P_D$) for a given False Alarm Probability ($P_{FA}$). The nature of the Q function dictates that, increasing the quantity under the square root increases the performance of the detector. The quantity $d^2 = \dfrac{1}{\tilde{\rho}^2}$ thus determines the performance of the detector. Since it is the ratio of the signal power to noise power, it is called the Signal to Noise Ratio (SNR).

#### 3.1.3 An Example and ROC Curves

Consider the step function $f(x)$ as described in the previous discussion. Let its Fourier coefficients be corrupted by complex additive Gaussian white noise of variance $\rho^2 = 1.5$. The resulting jump function approximation is shown in Fig 6. For a visual understanding of the amount of noise, the Fourier reconstruction of the step function is also plotted in Fig 7.

From Eqs. 6 and 7, it is clear that the Probability of Detection, $P_D$ and the False Alarm Probability, $P_{FA}$ are functions of the threshold $\gamma$. Depending on requirements, the detector may be operated at any threshold between the two bounding points $(P_{FA}, P_D) = (0, 0)$ and $(P_{FA}, P_D) = (1, 1)$. These two points correspond to the two extreme cases where the detector is either "always off" - $(P_{FA}, P_D) = (0, 0)$ or "always on" - $(P_{FA}, P_D) = (1, 1)$. Hence, the curve plotting the $(P_{FA}, P_D)$ pair for the full range of thresholds is called a Receiver Operating Characteristic (ROC) curve. The ROC curve helps in choosing a suitable operating point for the detector and in comparing the performance of different detectors. Eq. 8 describes the ROC curve for the detector in discussion. This curve may also be obtained by Monte Carlo simulation methods, where each $(P_{FA}, P_D)$ pair on the ROC curve is obtained by counting the number of times the test statistic (under either

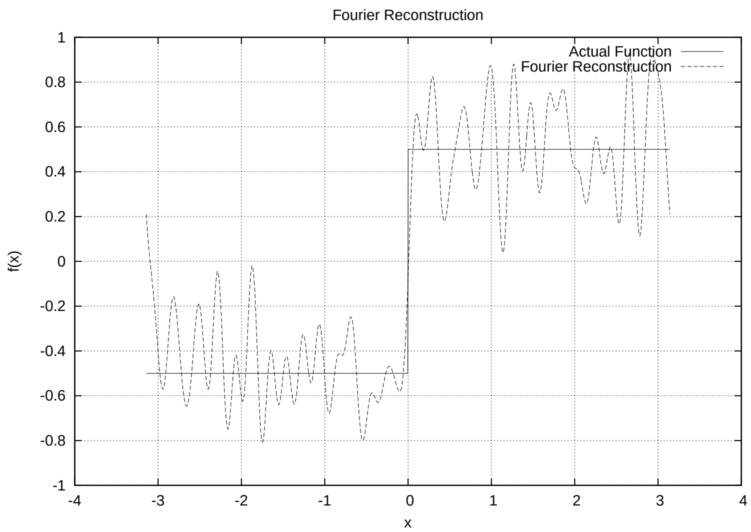


Figure 7: Partial Sum Fourier Reconstruction ($N = 32$, $\rho^2 = 1.5$)

hypothesis) exceeds the associated threshold. Fig. 8 shows the ROC curve for the detector under discussion.

## 3.2 Vector Case

### 3.2.1 Detector Design

Consider now a detector which accepts a data vector of the form $\mathbf{Y} = [\mathbf{y}_1\,\mathbf{y}_2\,...\,\mathbf{y}_k]^T$ where $\mathbf{y}_i$ is a point in the jump function approximation, $S_N^\sigma[\mathbf{g}](x_i)$. As in 3.1.1, we statistically describe $\mathbf{Y}$ under both hypotheses.

$$\mathcal{H}_0 : \quad \mathbf{Y} = \mathbf{N}$$

$$\mathcal{H}_1 : \quad \mathbf{Y} = S + \mathbf{N}$$

As before, in the absence of an edge, the contributing factor is noise and, in the presence of an edge, noise corrupts the true signal vector $S$. Here, $\mathbf{N}$ is multivariate Gaussian of zero mean and covariance matrix $C_\mathbf{N}$ (Section 2). $S$ is the signal vector and $S = [S_N^\sigma[f](x_1)\,S_N^\sigma[f](x_2)\,...\,S_N^\sigma[f](x_k)]^T$ Now,

$$f_\mathbf{Y}(Y|\mathcal{H}_0) = \mathcal{N}[0, C_\mathbf{N}]$$

$$f_\mathbf{Y}(Y|\mathcal{H}_1) = \mathcal{N}[S, C_\mathbf{N}]$$

Applying the Neyman Pearson criterion,

$$\rightarrow \mathcal{H}_1 : \quad \frac{f_\mathbf{Y}(Y|\mathcal{H}_1)}{f_\mathbf{Y}(Y|\mathcal{H}_0)} > \gamma$$

$$\frac{\frac{1}{(2\pi C_\mathbf{N})^{k/2}} \exp\left[-\frac{1}{2}(\mathbf{Y} - S)^T C_\mathbf{N}^{-1}(\mathbf{Y} - S)\right]}{\frac{1}{(2\pi C_\mathbf{N})^{k/2}} \exp\left[-\frac{1}{2}\mathbf{Y}^T C_\mathbf{N}^{-1}\mathbf{Y}\right]} > \gamma$$

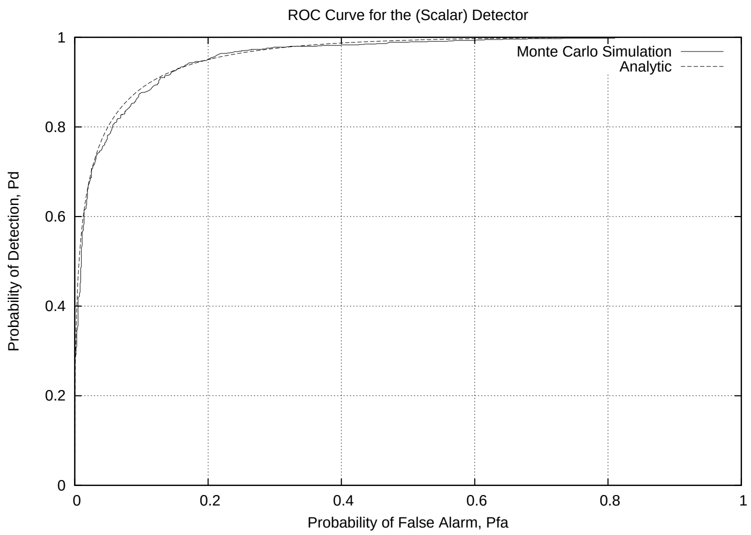


Figure 8: ROC Curve - Scalar Detector ($N = 32$, Polynomial Concentration Factor, $\rho^2 = 1.5$)

$$\exp\left[-\frac{1}{2}(\mathbf{Y}-S)^T C_{\mathbf{N}}^{-1}(\mathbf{Y}-S)\right]\exp\left[\frac{1}{2}\mathbf{Y}^T C_{\mathbf{N}}^{-1}\mathbf{Y}\right] > \gamma$$

$$\exp\left[-\frac{1}{2}\left(\mathbf{Y}^T C_{\mathbf{N}}^{-1}\mathbf{Y} - S^T C_{\mathbf{N}}^{-1}\mathbf{Y} - \mathbf{Y}^T C_{\mathbf{N}}^{-1} S + S^T C_{\mathbf{N}}^{-1} S - Y^T C_{\mathbf{N}}^{-1} Y\right)\right] > \gamma$$

$$\exp\left[S^T C_{\mathbf{N}}^{-1}\mathbf{Y} - \frac{1}{2} S^T C_{\mathbf{N}}^{-1} S\right] > \gamma$$

Incorporating the data independent term $\exp\left[-\frac{1}{2} S^T C_{\mathbf{N}}^{-1} S\right]$ into the threshold

$$\begin{aligned} \exp\left[S^T C_{\mathbf{N}}^{-1}\mathbf{Y}\right] &> \bar{\gamma} \\ \text{or, } \rightarrow \mathcal{H}_1: \quad S^T C_{\mathbf{N}}^{-1}\mathbf{Y} &> \dot{\gamma} \text{ where } \dot{\gamma} = \ln\bar{\gamma} \end{aligned} \tag{9}$$

### 3.2.2 Performance of the Detector

The test statistic as given by Eq. 9 is $TS = S^T C_{\mathbf{N}}^{-1}\mathbf{Y}$. Obtaining an analytic expression for the ROC curve is complicated by the presence of the covariance matrix. A popular method to simplify the analysis, and indeed, implement the detector is to perform a whitening transform, i.e., premultiply the data and signal vectors by a whitening matrix $W$ so that the resulting noise structure is white. If $\mathbf{Z}$ be the modified data vector and $M$ be the modified signal vector,

$$Z = W\mathbf{Y}$$

$$M = WS$$

Here, $W$ is chosen to be equal to $\sqrt{\Lambda^{-1}}U$, where $UC_{\mathbf{N}}U^T = \Lambda$. In other words, $U$ diagonalizes $C_{\mathbf{N}}$ while $W = \sqrt{\Lambda^{-1}}U$ reduces it to the identity matrix. Hence,

$$C_{\mathbf{N}'} = WC_{\mathbf{N}}W^T = I$$

The modified test statistic now becomes,

$$TS = M^T C_{\mathbf{N}'}^{-1} \mathbf{Z} = M^T I \mathbf{Z} = M^T \mathbf{Z}$$

Now, we can write the distribution of the test statistic under either hypothesis.

Under $\mathcal{H}_0$:

$$\mathbf{Z} = W\mathbf{N} = \mathbf{N}^{'}$$

Hence, $TS_{\mathcal{H}_0} = M^T \mathbf{N}^{'}$. This is a linear combination of independent Gaussian random variables. Since $\mathbf{N}^{'}$ remains zero mean, the mean of the linear combination is zero. The variance takes the form $m_1^2 + m_2^2 + ... + m_k^2$. Hence,

$$TS_{\mathcal{H}_0} \sim \mathcal{N}[0, ||M||^2]$$

Under $\mathcal{H}_1$:

$$\mathbf{Z} = W(S + \mathbf{N}) = M + \mathbf{N}^{'}$$

Hence, $TS_{\mathcal{H}_1} = M^T(M + \mathbf{N}^{'})$. This is still a linear combination of independent Gaussian random variables. The mean in this case is $||M||^2$ and the variance, as before, is $||M||^2$.

$$TS_{\mathcal{H}_1} \sim \mathcal{N}[||M||^2, ||M||^2]$$

Following the same steps as in the scalar case,

$$\begin{aligned} P_{FA} &= \int_{\dot{\gamma}}^{\infty} p\left(TS_{\mathcal{H}_0}(y)\right) dy \\ &= \int_{\dot{\gamma}}^{\infty} \frac{1}{\sqrt{2\pi ||M||^2}} \exp\left[-\frac{y^2}{2||M||^2}\right] dy \\ &= Q\left(\frac{\dot{\gamma}}{||M||}\right) \end{aligned} \tag{10}$$

$$\begin{aligned} P_D &= \int_{\dot{\gamma}}^{\infty} p\left(TS_{\mathcal{H}_1}(y)\right) dy \\ &= \int_{\dot{\gamma}}^{\infty} \frac{1}{\sqrt{2\pi ||M||^2}} \exp\left[-\frac{\left(y - ||M||^2\right)^2}{2||M||^2}\right] dy \\ &= Q\left(\frac{\dot{\gamma} - ||M||^2}{||M||}\right) \end{aligned} \tag{11}$$

Using Equations 10 and 11, we may write

$$\begin{aligned} P_D &= Q\left(\frac{Q^{-1}(P_{FA})||M|| - ||M||^2}{||M||}\right) \\ P_D &= Q\left(Q^{-1}(P_{FA}) - \sqrt{||M||^2}\right) \end{aligned} \tag{12}$$

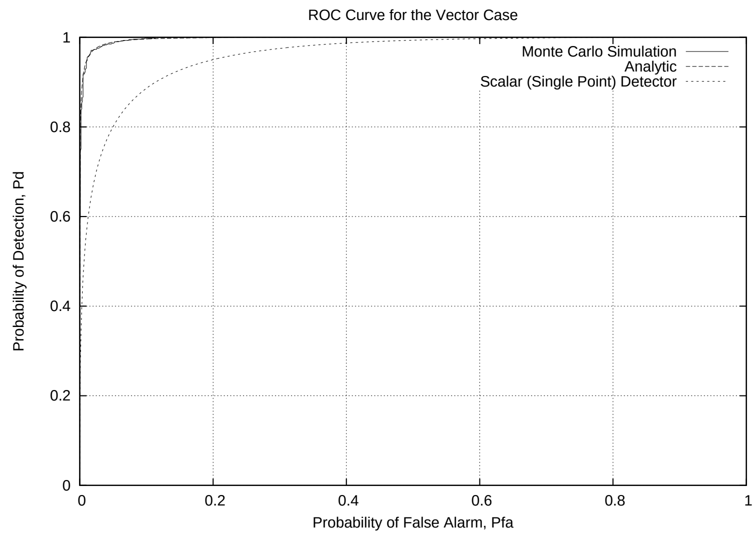


Figure 9: ROC Curve - 5 Point Detector ($N = 32$, Polynomial Concentration Factor, $\rho^2 = 1.5$)

As before, for a given $P_{FA}$, the performance is determined by the quantity $||M||^2$. But,

$$\begin{aligned} ||M||^2 &= M^T M \\ &= (WS)^T (WS) \\ &= S^T W^T W S \end{aligned}$$

Substituting [4] for $W^T W$, we get

$$||M||^2 = S^T C_{\mathbf{N}}^{-1} S \tag{13}$$

Fig. 9 shows the ROC for a detector which uses 5 points picked from the jump function approximation of a Polynomial concentration factor. These points were picked symmetrically from the local maxima/minima of the response. For comparison, the ROC of the scalar detector is also plotted. The gain in performance by using 5 points against a single point is about 4 dB [5].

[4] $W^T W = (\sqrt{\Lambda^{-1}}U)^T(\sqrt{\Lambda^{-1}}U) = U^T\sqrt{\Lambda^{-1}}\sqrt{\Lambda^{-1}}U = U^T\Lambda^{-1}U$
Since $U$ is unitary, $UC_{\mathbf{N}}U^T = \Lambda \Rightarrow C_{\mathbf{N}} = U^T\Lambda U$ and $U^T\Lambda^{-1}U = C_{\mathbf{N}}^{-1}$

[5] $10\log_{10}\left(\frac{||M||^2}{d^2}\right) = 10\log_{10}\left(\frac{15.567}{6.191}\right) \approx 4dB$

## References


[1] *Fundamentals of Statistical Signal Processing - Detection Theory*, chapter 3. Prentice Hall Signal Processing Series, 1993.

[2] Anne Gelb and Eitan Tadmor. Detection of edges in spectral data. *Applied and Computational Harmonic Analysis*, 1999.

[3] Anne Gelb and Eitan Tadmor. Detection of edges in spectral data II - Nonlinear Enhancement. *SIAM Journal in Numerical Analysis*, 2000.

[4] Anne Gelb and Eitan Tadmor. Adaptive edge detectors for piecewise smooth data based on the minmod limiter. *Journal of Scientific Computing*, 2006.